

Dynamical Properties of One-Dimensional Multicomponent Quantum Liquids in Metallic Phase

Satoshi MIYASHITA * , Akira KAWAGUCHI and Norio KAWAKAMI

Department of Applied Physics, Osaka University, Suita, Osaka 565-0871, Japan

(Received October 26, 2018)

We investigate low-energy dynamical properties of one-dimensional multicomponent quantum liquids with the short-range interaction as well as the $1/x$ -type long-range interaction. By calculating the single-particle spectrum and the dynamical spin susceptibility by means of the bosonization method, we discuss how the orbital degeneracy and the band splitting affect the dynamical response functions. The effect of the long-range interaction is also addressed. Although the long-range interaction suppresses charge fluctuations, it effectively enhances spin fluctuations via the formation of the Wigner crystal.

KEYWORDS: Tomonaga-Luttinger liquid, dynamical responses, orbital degeneracy, long-range interaction

§1. Introduction

Low-energy excitations in one-dimensional (1D) correlated electron systems with the short-range interaction are described by collective charge and spin fluctuations. This class of quantum liquids is referred to as the Tomonaga-Luttinger (TL) liquid.^{1,2,3)} Recently, dynamical properties of 1D electron systems have been studied extensively by various experimental methods, *e.g.* angle resolved photoemission spectroscopy (ARPES),^{4,5)} NMR,^{6,7,8)} etc. In particular, the spin-charge separation inherent in 1D electron systems was observed in the single-particle spectrum via the ARPES measurements,^{4,5)} and typical power-law behaviors in spin correlation functions were observed in the temperature dependence of the NMR relaxation rate^{9,10,11)} in various 1D compounds.^{6,7,8)}

More recently, the effect of the orbital degrees of freedom has attracted renewed interest in correlated electron systems. Such orbital effects are indeed important in 1D. For example, in 1D correlated electron systems at quarter-filling, such as $\text{Na}_2\text{Ti}_2\text{Sb}_2\text{O}^{12)}$ and NaV_2O_5 ,^{13,14,15,16,17,18)} the effective orbital degrees of freedom are essential to understand the correct low-temperature properties. In this connection, the 1D multicomponent spin-orbital model has been extensively

* E-mail : satoshi@tp.ap.eng.osaka-u.ac.jp

studied analytically^{19, 20, 21, 22, 23, 24, 25)} and numerically.^{26, 27)} However, dynamical correlation functions have not been studied systematically so far, except for exactly solvable $1/r^2$ -models.^{28, 29, 30)}

It is usually assumed that the Coulomb interaction is well screened, and the resulting interaction is short-ranged in the TL liquid. However, this is not always the case for quasi-1D systems, since the screening effect due to adjacent chains is not efficient enough in some cases, leading to the bare long-range interaction. The resulting quantum liquid is a 1D analog of the Wigner crystal, which exhibits quite different properties from those of the TL liquid.^{31, 32, 33)}

In this paper, we investigate the effect of the orbital degeneracy on low-energy dynamical properties of the TL liquid by employing the bosonization method for the two-orbital electron model. We also clarify how the long-range interaction affects dynamical properties via the formation of the 1D Wigner crystal. This paper is organized as follows. In §2, we introduce the model and derive a low-energy effective Hamiltonian in the bosonized form. In §3, we investigate the orbital effects on the TL liquid with the short-range interaction and then in §4 discuss the effect of the long-range interaction on the low-energy properties of the system. A brief summary is given in the last section.

§2. Low-Energy Effective Hamiltonian

In this section, we outline the derivation of a low-energy effective Hamiltonian in the bosonized form. We start with the 1D two-orbital Hubbard model with the band splitting Δ ,

$$\begin{aligned} \mathcal{H} = & -t \sum_{j a \sigma} (c_{j a \sigma}^\dagger c_{j+1 a \sigma} + h.c.) \\ & + \frac{1}{2} \sum_{i, j} \sum_{a, b} \sum_{\sigma, \sigma'} U(x_i - x_j) n_{i a \sigma} n_{j b \sigma'} (1 - \delta_{i, j} \delta_{a, b} \delta_{\sigma, \sigma'}) \\ & - \Delta \sum_j [(n_{j1\uparrow} + n_{j1\downarrow}) - (n_{j2\uparrow} + n_{j2\downarrow})], \end{aligned} \quad (1)$$

where $c_{j a \sigma}^\dagger$ creates an electron with the orbital index $a = 1$ (lower band), 2 (upper band) and spin $\sigma = \uparrow, \downarrow$ at the j -th site. In the absence of the band splitting, $\Delta=0$, the above model corresponds to the SU(4) symmetric Hubbard model. For simplicity, we have neglected the Hund-rule coupling between different orbitals, which are irrelevant in the following discussions in the TL liquid phase.

Passing to the continuum limit, we derive a low-energy effective Hamiltonian in terms of the slowly varying right- and left-going Fermi fields $c_{j a \sigma}^{(+)}$ and $c_{j a \sigma}^{(-)}$, which are related to the original lattice operator as

$$c_{j a \sigma} \sim \sqrt{a_0} \left[e^{i k_F^{(a)} j a_0} c_{j a \sigma}^{(+)} + e^{-i k_F^{(a)} j a_0} c_{j a \sigma}^{(-)} \right], \quad (2)$$

where a_0 is the lattice spacing and $k_F^{(1)}$ ($k_F^{(2)}$) is the Fermi momentum of the lower (upper) band. Since we are interested in a metallic phase with the repulsive interaction, we are left with only forward scatterings. By using the Fourier decompositions $c_{j a \sigma}^{(r)} = \frac{1}{\sqrt{N}} \sum_p e^{-i p j a_0} c_{r p a \sigma}$ ($r=+$ or $-$),

the Hamiltonian (1) is rewritten as

$$\begin{aligned} \mathcal{H} = & \frac{\pi}{L} \sum_{p,a,\sigma} v_F^{(a)} [\rho_{+a\sigma}(p)\rho_{+a\sigma}(-p) + \rho_{-a\sigma}(-p)\rho_{-a\sigma}(p)] \\ & + \frac{1}{2L} \sum_{\substack{p,a,b \\ \sigma,\sigma'}} U(p) [\rho_{+a\sigma}(p) + \rho_{-a\sigma}(p)] [\rho_{+b\sigma'}(-p) + \rho_{-b\sigma'}(-p)], \end{aligned} \quad (3)$$

where $\rho_{ra\sigma}(p) = \sum_k c_{rk+pa\sigma}^\dagger c_{rka\sigma}$ are the density operators satisfying the bosonic commutation relation, and $v_F^{(a)} = a_0 t \sin(k_F^{(a)} a_0)$ is the Fermi velocity of the lower band ($a = 1$) or the upper band ($a = 2$). We have four kinds of bosonic fields, $\rho_{r1\uparrow}$, $\rho_{r1\downarrow}$, $\rho_{r2\uparrow}$ and $\rho_{r2\downarrow}$, which are converted via a unitary transformation to the new bosonic fields corresponding to the 'charge'(c), 'spin'(s), 'orbital'(o) and 'spin-orbital'(so) sectors,

$$\begin{pmatrix} \rho_{rc}(p) \\ \rho_{rs}(p) \\ \rho_{ro}(p) \\ \rho_{rso}(p) \end{pmatrix} = \frac{1}{2} \begin{pmatrix} 1 & 1 & 1 & 1 \\ 1 & -1 & 1 & -1 \\ 1 & 1 & -1 & -1 \\ 1 & -1 & -1 & 1 \end{pmatrix} \begin{pmatrix} \rho_{r1\uparrow}(p) \\ \rho_{r1\downarrow}(p) \\ \rho_{r2\uparrow}(p) \\ \rho_{r2\downarrow}(p) \end{pmatrix}. \quad (4)$$

Moreover, when the band splitting takes a finite value, it is convenient to use the new basis for the charge and orbital sectors,

$$\begin{pmatrix} \rho_{+c} + \rho_{-c} \\ \rho_{+o} + \rho_{-o} \end{pmatrix} = \begin{pmatrix} \xi_1(p) & -\xi_3(p) \\ \xi_2(p) & \xi_1(p) \end{pmatrix} \begin{pmatrix} \tilde{\rho}_{+c} + \tilde{\rho}_{-c} \\ \tilde{\rho}_{+o} + \tilde{\rho}_{-o} \end{pmatrix}, \quad (5)$$

where

$$\xi_1(p) = \cos[\alpha(p)], \quad (6)$$

$$\xi_2(p) = y(p) \sin[\alpha(p)], \quad (7)$$

$$\xi_3(p) = \frac{1}{y(p)} \sin[\alpha(p)]. \quad (8)$$

The explicit formulae for $y(p)$ and $\alpha(p)$ are given in Appendix. Note that when two orbitals are degenerate ($\Delta=0$), we have $\alpha(p) = 0$, so that $\xi_1 = 1$ and $\xi_2 = \xi_3 = 0$.

Consequently, we end up with the Hamiltonian,

$$\mathcal{H} = \frac{\pi}{2L} \sum_{\nu} \sum_p \tilde{v}_{\nu}(p) \left\{ \frac{1}{\tilde{K}_{\nu}(p)} [\tilde{\rho}_{+\nu}(p) + \tilde{\rho}_{-\nu}(p)]^2 + \tilde{K}_{\nu}(p) [\tilde{\rho}_{+\nu}(p) - \tilde{\rho}_{-\nu}(p)]^2 \right\}, \quad (9)$$

where the velocities and the TL parameters are summarized in Appendix.

This completes the derivation of a low-energy effective theory of 1D correlated electrons with two orbitals. Though we have outlined the way in terms of the Hubbard model, the resulting formula can be applied to generic two-band models in a metallic phase.

Before closing this section, some comments are in order for the formula (9). In terms of the spin and spin-orbital basis, the velocities read $\tilde{v}_s = v_F^{(1)}$ and $\tilde{v}_{so} = \tilde{v}_F^{(2)}$. Moreover, we should set $\tilde{K}_s = \tilde{K}_{so} = 1$ according to SU(2) symmetry required for these excitation modes.

§3. Multicomponent Tomonaga-Luttinger Liquid

We first consider the system with the short-range interaction and discuss how the orbital degrees of freedom affect the dynamical response functions. When the interaction is short-ranged (δ -function), we set all the parameters, $\tilde{v}_\nu(p)$ and $\tilde{K}_\nu(p)$, independent of the momentum p . We employ the t - J model as a microscopic model to give the values of $\tilde{v}'_{c,o}$ and $\tilde{K}'_{c,o}$. Furthermore, if we make use of the integrable supersymmetric t - J model,^{19,34,35,36} where the hopping t and the spin exchange coupling J satisfies the relation, $t = J$, the above TL parameters can be determined by the Bethe ansatz method combined with conformal field theory. This model is somewhat special, but it can well describe general properties of the doped spin-orbital model, as far as we are concerned with a metallic system near the insulating phase.

We first derive the single-particle Green function^{37,38,39,40} for the TL liquid with orbital degeneracy, which is defined as

$$\begin{aligned}\tilde{G}_{ra\sigma}(x, t) &= -i\Theta(t)\langle[\psi_{ra\sigma}(x, t), \psi_{ra\sigma}^\dagger(0, 0)]_+\rangle \\ &= -i\Theta(t)[G_{ra\sigma}^<(x, t) + G_{ra\sigma}^<(-x, -t)],\end{aligned}\quad (10)$$

where

$$G_{ra\sigma}^<(x, t) = \langle \psi_{ra\sigma}(x, t) \psi_{ra\sigma}^\dagger(0, 0) \rangle, \quad (11)$$

and $G_{ra\sigma}^>(x, t)$ is defined similarly. The Fermi field is written down as

$$\psi_{ra\sigma} = \lim_{a_0 \rightarrow 0} \frac{\eta_{ra\sigma}}{\sqrt{2\pi a_0}} \exp\left(-\frac{i}{2} \sum_\nu \left[r\tilde{\phi}_\nu - \tilde{\theta}_\nu\right]\right), \quad (12)$$

where $\eta_{ra\sigma}$ is the Klein factor, which ensures the anti-commutation relation between the right- and left-going electrons. The above two phase fields are

$$\tilde{\phi}_\nu(x) = -\frac{i\pi}{L} \sum_p \frac{1}{p} e^{-\frac{1}{2}a_0|p| - ipx} \xi_{\phi a\sigma}^\nu(p) [\tilde{\rho}_{+\nu}(p) + \tilde{\rho}_{-\nu}(p)], \quad (13)$$

$$\tilde{\theta}_\nu(x) = \frac{i\pi}{L} \sum_p \frac{1}{p} e^{-\frac{1}{2}a_0|p| - ipx} \xi_{\theta a\sigma}^\nu(p) [\tilde{\rho}_{+\nu}(p) - \tilde{\rho}_{-\nu}(p)], \quad (14)$$

where

$$\begin{cases} \xi_{\phi a\sigma}^c(p) = \xi_1(p) + (-1)^{a+1} \xi_2(p) \\ \xi_{\theta a\sigma}^c(p) = \xi_1(p) + (-1)^{a+1} \xi_3(p) \end{cases}, \quad (15)$$

$$\begin{cases} \xi_{\phi_{a\sigma}}^o(p) = -\xi_3(p) + (-1)^{a+1}\xi_1(p) \\ \xi_{\theta_{a\sigma}}^o(p) = -\xi_2(p) + (-1)^{a+1}\xi_1(p) \end{cases}, \quad (16)$$

$$\begin{cases} \xi_{\phi_{a\sigma}}^s(p) = \xi_{\theta_{a\sigma}}^s(p) = \frac{\sigma}{\sqrt{2}}\{1 + (-1)^{a+1}\} \\ \xi_{\phi_{a\sigma}}^{so}(p) = \xi_{\theta_{a\sigma}}^{so}(p) = \frac{\sigma}{\sqrt{2}}\{1 - (-1)^{a+1}\} \end{cases}. \quad (17)$$

Note that $\tilde{\theta}_\nu$ is the bosonic field conjugate to $\tilde{\phi}_\nu$, which satisfies $[\tilde{\phi}_\nu(x), \tilde{\theta}_{\nu'}(x')] = i\frac{\pi}{2}\delta_{\nu,\nu'}\text{sgn}(x-x')$.

Inserting these expressions into the Green function, we have

$$G_{ra\sigma}^<(x, t) = \frac{1}{2\pi} \prod_{\substack{\nu=c,s, \\ o,so}} \frac{e^{-i\frac{\pi}{2}2\tilde{\Delta}_\nu^+ \text{sgn}(x+\tilde{v}_\nu t)} e^{i\frac{\pi}{2}2\tilde{\Delta}_\nu^- \text{sgn}(x-\tilde{v}_\nu t)} \left(\frac{\pi}{\beta\tilde{v}_\nu}\right)^{2\tilde{x}_\nu}}{\left|\sinh\left[\frac{\pi}{\beta\tilde{v}_\nu}(x+\tilde{v}_\nu t)\right]\right|^{2\tilde{\Delta}_\nu^+} \left|\sinh\left[\frac{\pi}{\beta\tilde{v}_\nu}(x-\tilde{v}_\nu t)\right]\right|^{2\tilde{\Delta}_\nu^-}}, \quad (18)$$

with $\beta = 1/k_B T$, where the conformal dimensions are given by

$$2\tilde{\Delta}_\nu^\pm = \frac{1}{16}[\tilde{K}_\nu \xi_{\phi_{a\sigma}}^\nu{}^2 + \xi_{\theta_{a\sigma}}^\nu{}^2 / \tilde{K}_\nu \mp 2r \xi_{\phi_{a\sigma}}^\nu \xi_{\theta_{a\sigma}}^\nu], \quad (19)$$

and the corresponding scaling dimensions are $\tilde{x}_\nu = \tilde{\Delta}_\nu^+ + \tilde{\Delta}_\nu^-$. For $\Delta=0$, we have $\xi_{\phi_{a\sigma}}^\nu = \xi_{\theta_{a\sigma}}^\nu = 1$, which gives the conformal dimensions for the SU(4) spin model.²⁰⁾ Equation (18) implies that the spin-charge-orbital separation occurs in elementary excitations, as should be expected for 1D electron systems. Note, however, that all these degrees of freedom are combined together to contribute to the single-particle Green function. Fourier transformation of (10) gives the single-particle spectrum, $G_{ra\sigma}(k, \omega)$.

Let us now investigate the single-particle spectrum by focusing on right-moving fermions ($r=+$). To see the effect of the orbital degeneracy, we first compare the spectral function of the single-orbital electron system (2-component TL liquid) with that of the two-orbital one (4-component TL liquid). The system has the dispersions, $\omega = \tilde{v}_\nu k$, so that the spectral function may have several peaks around $\omega = \tilde{v}_\nu k$ at finite temperatures. We use the parameters which are derived from the exact solution of the multicomponent supersymmetric t - J model^{19,22)} near the Mott insulator in order to parameterize the velocities and the TL parameters as a function of the band splitting. For the case of single- and two-orbital TL liquids, we set $\tilde{v}_s = 2\pi/n$, $\tilde{K}_c = 1/n$ ($n = 2$ or 4) whereas $\tilde{K}_s = 1$ is fixed due to SU(2) or SU(4) symmetry. We set a small value for the charge velocity ($\tilde{v}_c = 0.1$) because we are interested in the vicinity of the Mott insulator. Note that we will measure the energy in the unit of the spin exchange coupling J .

We show the results for the TL liquid with and without orbital degeneracy in Fig. 1. At high temperatures, all the kinds of excitations show over-damped behaviors in which the spectral weight is distributed broadly around $\omega \sim 0$. This is valid both for the single- and two-orbital models. As the temperature decreases, the peak structure of the spectrum is gradually developed around each mode of elementary excitations. In the single-orbital case, the peak around the charge mode

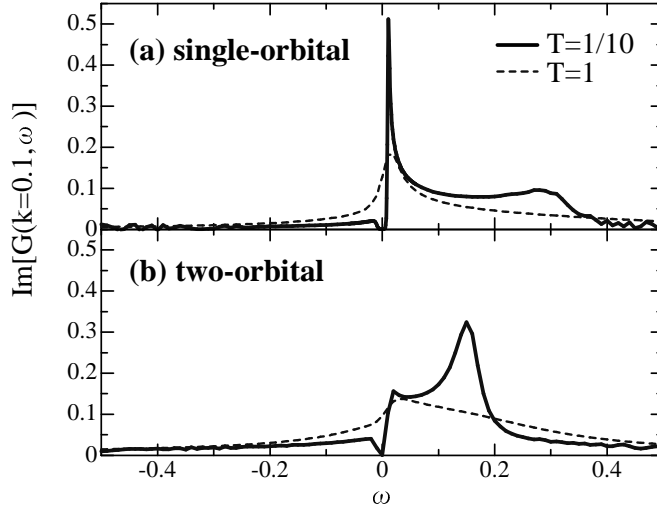


Fig. 1. Single-particle spectrum for the TL liquid; (a) SU(2) single-orbital case, $\tilde{v}_c=0.1$, $\tilde{v}_s=\pi$, (b) SU(4) two-orbital case, $\tilde{v}_c=0.1$, $\tilde{v}_s=\tilde{v}_o=\tilde{v}_{so}=\pi/2$.

($\omega\sim 0.01$) is enhanced more prominently than that for the spin mode ($\omega\sim 0.3$) at low temperatures. On the other hand, in the two-orbital case, the peak structure for the charge mode ($\omega\sim 0.01$) is rather suppressed, while that for the spin mode ($\omega\sim 0.17$) is enhanced. This is understood by looking at the zero-temperature behavior of the spectrum. At $T=0$, the above spectral function shows power-law divergence near each excitation mode as,

$$\text{Im}G(k, \omega) \sim |\omega - \tilde{v}_\nu k|^{-2\tilde{\Delta}_\nu^-}, \quad \omega > 0, \quad (20)$$

for the mode specified by ν , where the corresponding critical exponents are listed in Table 3. It is seen that the spin exponent $2\tilde{\Delta}_s^-$ is increased in the two-orbital case due to the orbital degeneracy, resulting in the enhanced peak structure. On the other hand, the charge exponent $2\tilde{\Delta}_c^-$ is decreased in the orbitally degenerate case, being consistent with the suppressed charge mode in Fig. 1(b). In this way, the orbital degeneracy affects not only the internal spin- and orbital-degrees of freedom but also the charge degrees of freedom, changing the structure of the spectral function rather considerably.

We now discuss the effect of the band splitting. The single-particle spectral function is shown for the band splitting $\Delta \simeq 0.6$ in Fig. 2, which should be compared with the case of $\Delta=0$ in Fig. 1(b). When the band splitting is present, the velocities take different values. We set these parameters as, $\tilde{v}_s \simeq 2.6$, $\tilde{v}_o \simeq 0.8$, $\tilde{v}_{so} \simeq 0.25$, $\tilde{K}_c = 1/n$, $\tilde{K}_o = 2/(n \times 0.436)$ ($n = 4$) according to the exact solution of the supersymmetric t - J model near the Mott insulator^{22,11)} and $\tilde{K}_s = \tilde{K}_{so} = 1$ due to the symmetry requirement. In order to clarify the properties of the spectrum, we glance at the critical exponents

Table I. Critical exponent of the single-particle spectrum.

	$2\tilde{\Delta}_c^-$	$2\tilde{\Delta}_s^-$	$2\tilde{\Delta}_o^-$	$2\tilde{\Delta}_{so}^-$
single-orbital	$\frac{9}{16}$	$\frac{1}{2}$	-	-
two-orbital ($\Delta=0$)	$\frac{25}{64}$	$\frac{3}{4}$	-	-
two-orbital ($\Delta \simeq 0.6$)				
upper band	0.563	0	0.072	$\frac{1}{2}$
lower band	0.250	$\frac{1}{2}$	0.540	0

again at zero temperature listed in Table 3. It is seen in Fig. 2 that the introduction of the band splitting alters the shape of the spectrum rather dramatically. Firstly, we notice that the peak structure of the charge sector ($\omega \sim 0.01$) is suppressed (enhanced) for the lower (upper) band in the presence of the band splitting. This is indeed seen from the change in the critical exponents; $2\tilde{\Delta}_c^-$ decreases (increases) for the lower (upper) band with the increase of the band splitting, which has a tendency to smear (pronounce) the singularity around $\omega = \tilde{v}_c k$ at $T = 0$. The remaining two peaks in the spectrum of the lower band in Fig. 2(b) are respectively identified with the contribution from the orbital ($\omega \sim 0.08$) and spin ($\omega \sim 0.26$) degrees of freedom. Note that the spin-orbital degrees of freedom do not contribute to the spectrum of the lower band. On the other hand, the spectrum shows a quite different behavior for the upper band (Fig. 2(a)). Namely, it has two peaks, which are mainly contributed by the charge and the spin-orbital ($\omega \sim 0.025$) sectors. As seen from the Table 3, the orbital sector also has a finite contribution, but its critical exponent is too small to make a visible peak structure around $T = 1/10$. In this way, the introduction of the band splitting brings about a considerable change in the profile of the spectral function, which is quite contrasted to that expected for the Fermi liquid system.

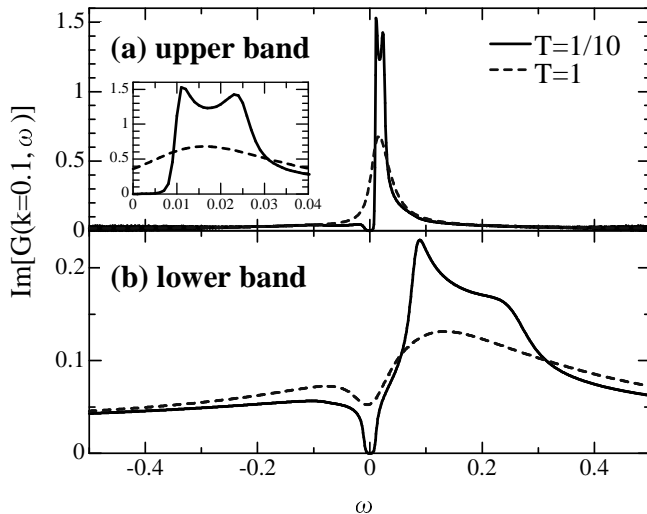


Fig. 2. Single-particle spectrum for the two-orbital TL liquid with the band splitting $\Delta \simeq 0.6$; $\tilde{v}_c = 0.1$, $\tilde{v}_s \simeq 2.6$, $\tilde{v}_o \simeq 0.8$, $\tilde{v}_{so} \simeq 0.25$, (a) upper band, (b) lower band.

We now turn to the dynamical spin susceptibility. We show the results calculated for $\text{Im}[\chi(k, \omega)]/\omega$ at and near the Mott insulator in Fig. 3. We also compare the results for the single- and two-orbital TL liquid ($\Delta=0$). As is clearly seen from the single-orbital case, a considerable amount of the spectral weight is transferred from the spin part to the charge part upon hole doping. This dramatic change is in contrast to our naive expectation that the charge excitation has little effect on the dynamical spin susceptibility. It is seen from Fig. 3(b) that this tendency is also the case for the two-orbital model, although the rate of the transferred weight is somehow small. These remarkable results imply that the NMR relaxation rate^{9,10,11,6,7,8}) may be possibly enhanced upon hole doping via a relaxation process mediated indirectly by low-energy charge channels. In Fig. 4 the effect of the band splitting is shown ($\Delta \simeq 0.6$). In this case, the spectral weight is transferred to low-energy charge and orbital modes upon hole doping.

We have so far seen that hole-doping induces the considerable transfer of the spectral weight to the low-energy charge mode in the dynamical spin susceptibility. In the following section, however,

this statement is shown to be valid only for the case of the short-range interaction, and a completely different behavior shows up for the long-range interaction model.

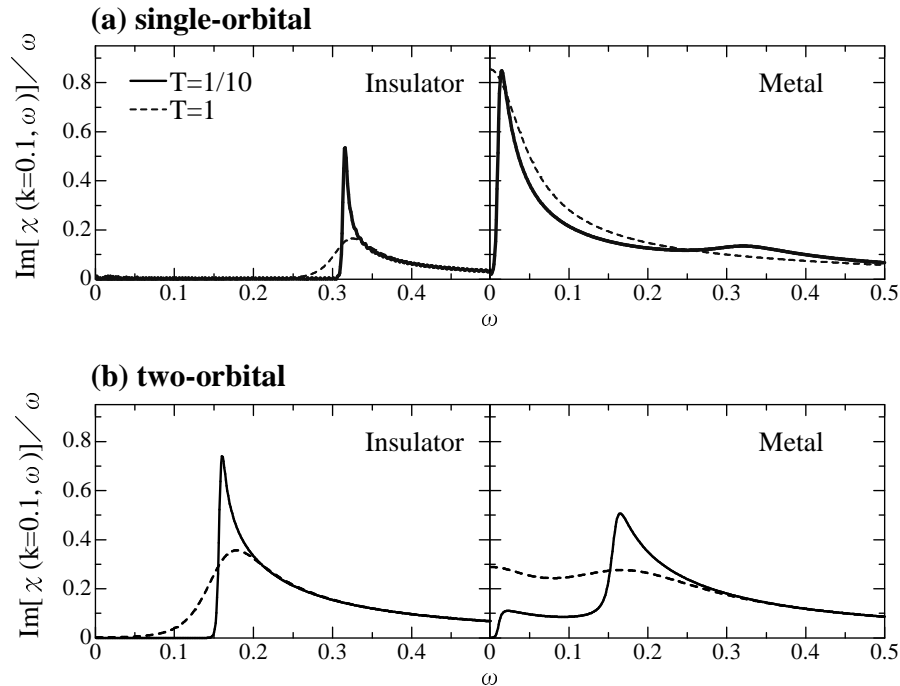


Fig. 3. Dynamical spin susceptibility at (left) and near (right) the Mott insulator; (a) SU(2) single-orbital case, $\tilde{v}_c=0.1$, $\tilde{v}_s=\pi$, (b) SU(4) two-orbital case, $\tilde{v}_c=0.1$, $\tilde{v}_s=\tilde{v}_o=\tilde{v}_{so}=\pi/2$. The momentum k measures the difference from $\pi/2$.

§4. Multicomponent Wigner Crystal

Let us now discuss the model with the long-range interaction, which may be important for quantum wires as well as carbon nanotubes. Also, for 1D highly correlated metallic systems close to the Mott insulator, the screening effect of the bare interaction may be rather poor, so that the long-range interaction is expected to play an important role. We will mainly focus on the latter case in the following discussions.

It is known that physical properties in the presence of the long-range interaction are quite different from those of the TL liquid. For example, the charge density correlation function has a power-law

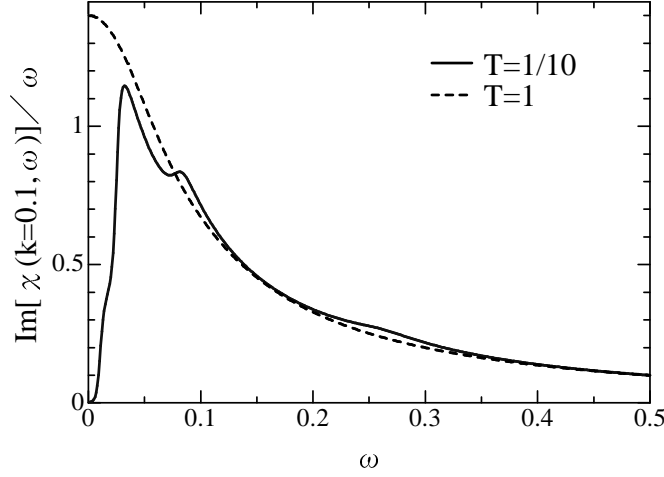


Fig. 4. Dynamical spin susceptibility for the two-orbital TL liquid in a metallic phase with the band splitting $\Delta \simeq 0.6$; $\tilde{v}_c=0.1$, $\tilde{v}_s \simeq 2.6$, $\tilde{v}_o \simeq 0.8$, $\tilde{v}_{so} \simeq 0.25$.

decay in the TL liquid with the dominant contribution of the $2k_F$ oscillating piece. When the long-range interaction is present, the correlation decays much more slowly, and thus causes a dominant $4k_F$ oscillating correlation. This is sometimes referred to as a 1D version of the Wigner crystal.³¹⁾

We introduce the following interaction in the Hamiltonian (1),

$$U(x) = \frac{e^2}{\epsilon \sqrt{x^2 + d^2}} \exp\left(-\frac{\sqrt{x^2 + d^2}}{\lambda}\right), \quad (21)$$

which smoothly interpolates the short-range interaction ($\lambda \rightarrow 0$) and the $1/x$ -type long-range interaction ($\lambda \rightarrow \infty$).³²⁾ Here the cut-off of $x \sim d$ is introduced to avoid a singular behavior at short distance. The Fourier transformation of (21) gives the modified Bessel function $K_0(x)$,

$$U(p) = \frac{2e^2}{\epsilon} K_0\left(\sqrt{p^2 + \lambda'^{-2}}\right), \quad (22)$$

where $\lambda' = \lambda/d$.

Even when the long-range Coulomb interaction is present, we can still diagonalize the Hamiltonian as far as the Umklapp and backward scatterings are irrelevant, leading to the formula (9). Note

that $\tilde{K}_c(p)$ and $\tilde{K}_o(p)$ now depend on the momentum p , whereas $\tilde{K}_s(p)$ and $\tilde{K}_{so}(p)$ are independent of p , whose value is restricted to $\tilde{K}_s(p)=\tilde{K}_{so}(p)=1$ as before.

To discuss the effect of the long-range interaction on the system with the orbital degeneracy, we again calculate the single-particle spectrum and the dynamical spin susceptibility. The single-particle Green function has the form,

$$G_{ra\sigma}^<(x, t) \sim \frac{1}{2\pi} \prod_{\mu=c,o} e^{-iC_\mu(x,t)} e^{-D_\mu(x,t)} \\ \times \prod_{\nu=s,so} \frac{e^{-i\frac{\pi}{2}2\tilde{\Delta}_\nu^+ \text{sgn}(x+\tilde{v}_\nu t)} e^{i\frac{\pi}{2}2\tilde{\Delta}_\nu^- \text{sgn}(x-\tilde{v}_\nu t)} \left(\frac{\pi}{\beta\tilde{v}_\nu}\right)^{2x_\nu}}{\left| \sinh \left[\frac{\pi}{\beta\tilde{v}_\nu} (x + \tilde{v}_\nu t) \right] \right|^{2\tilde{\Delta}_\nu^+} \left| \sinh \left[\frac{\pi}{\beta\tilde{v}_\nu} (x - \tilde{v}_\nu t) \right] \right|^{2\tilde{\Delta}_\nu^-}}, \quad (23)$$

where

$$C_\mu(x, t) = \int_0^\infty dp \frac{e^{-\alpha' p}}{p} \{2\tilde{\Delta}_\mu^+(p) \sin[\{x + \tilde{v}_\mu(p)t\} p] + 2\tilde{\Delta}_\mu^-(p) \sin[\{x - \tilde{v}_\mu(p)t\} p]\}, \quad (24)$$

$$D_\mu(x, t) = \int_0^\infty dp \frac{e^{-\alpha' p}}{p} (1 + 2n_p) \\ \times \{2\tilde{\Delta}_\mu^+(p) (1 - \cos[\{x + \tilde{v}_\mu(p)t\} p]) + 2\tilde{\Delta}_\mu^-(p) (1 - \cos[\{x - \tilde{v}_\mu(p)t\} p])\}, \quad (25)$$

with $\alpha'=a_0/d$ and $n_p=1/[\exp\{\tilde{v}_\mu(p)p/k_B T\}-1]$. In contrast to the short-range case, we cannot integrate the charge as well as the orbital parts analytically, so that we evaluate these integrals numerically.

We investigate three cases for which the range of the interaction is long ($\lambda'=10^4$), intermediate ($\lambda'=1$), and short ($\lambda'=10^{-2}$). As the long-range interaction has no essential effects on the spin velocity so it is given by that of the short-range case. We show the momentum-dependence of the charge velocity $v_c(p)$ and the TL parameter $K_c(p)$ calculated for the single-orbital case are shown in Fig. 5, which are scaled so as to properly reproduce $\tilde{v}_c=0.1$ and $\tilde{K}_c=1/2$ in the case of the short-range interaction. It is seen that when the long-range interaction is present, they are strongly dependent on p in the small p region.

The single-particle spectrum for the single- as well as two-orbital models is shown in Fig. 6, from which we can see how the spectrum changes its profile in the presence of the long-range interaction. In the single-orbital case shown in Fig. 6(a), both peaks coming from the charge ($\omega\sim 0.01$) and spin sectors ($\omega\sim 0.3$) are gradually suppressed as the interaction becomes long-ranged (large λ'). This means that the long-range interaction smoothly drives the system from the TL liquid to the 1D Wigner crystal. In Fig. 6(b), we show the two-orbital case without the band splitting ($\Delta=0$). Although the spectral function is affected considerably by the orbital degeneracy in the short-range

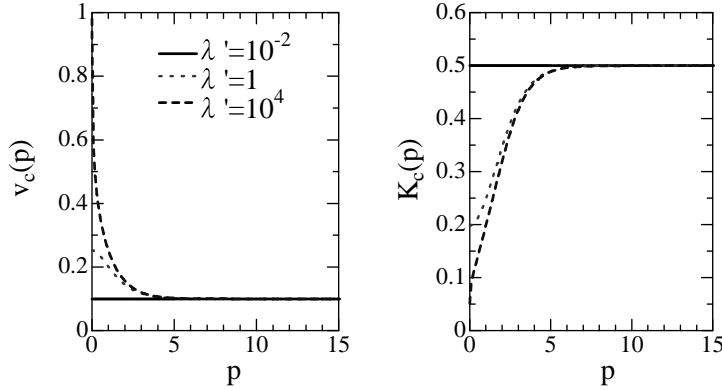


Fig. 5. Charge velocity $v_c(p)$ and TL parameter $K_c(p)$ for the single-orbital model with the long-range interaction.

interaction, the spectrum loses such characteristic features as the interaction becomes long-ranged. Such smearing effect of the spectral function is also seen for the case with the band splitting. The single-particle spectrum of the lower and upper bands is shown for $\Delta \simeq 0.6$ in Fig. 7. Therefore, as long as the single-particle spectrum is concerned, we would conclude that the long-range interaction obscures not only the charge mode but also the other spin and orbital modes in the 1D quantum liquids. However, this naive conclusion is misleading, which should not correctly capture the effect of the long-range interaction.

To clarify the above point, let us consider the dynamical spin susceptibility. In Fig. 8, we show how the long-range interaction affects the dynamical spin susceptibility with and without the orbital degeneracy. As is the case for the single-particle spectrum, the peak structure for the charge sector is suppressed as the interaction becomes long-ranged. However, it should be noticed that the peak structure due to the internal spin and orbital degrees of freedom is *enhanced* as the long-range

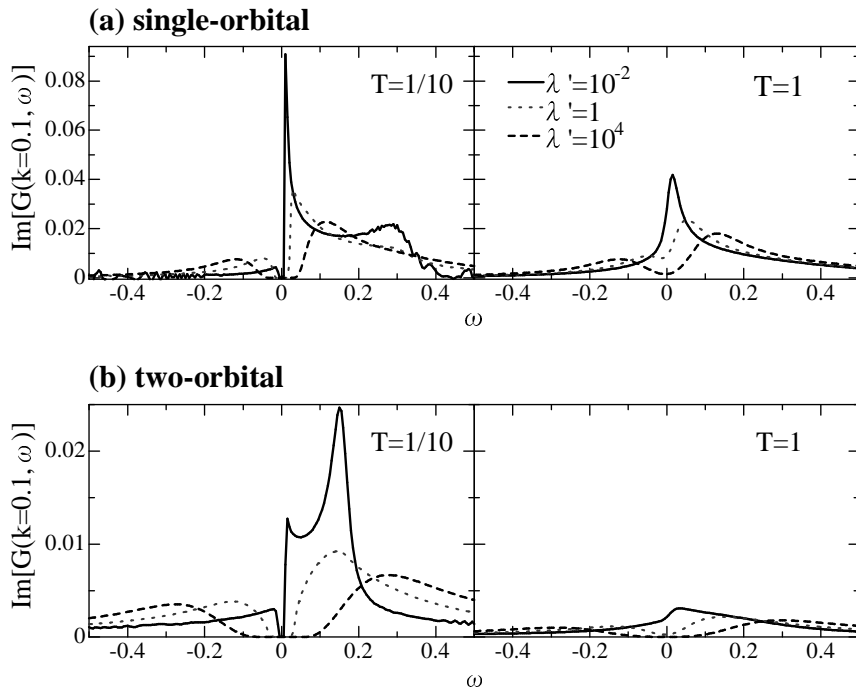


Fig. 6. Single-particle spectrum for (a) single-orbital model ($v_s = \pi$) and (b) two-orbital model ($v_s = v_o = v_{so} = \pi/2$). The range of the interaction is changed systematically by modifying λ' .

interaction is introduced, as clearly seen in Fig. 8. This characteristic behavior is quite contrasted to the results of the single-particle spectrum discussed above. The origin of the enhancement is rather clear; i.e. the long-range interaction drives the system to the 1D Wigner crystal, which almost freezes the charge degrees of freedom and thereby enhances the spin fluctuations effectively. When the single-particle spectrum is considered, such enhanced spin fluctuations are again masked by the charge excitations which are accompanied by an electron-like excitation.

Therefore, we come to the conclusion that the internal spin and orbital fluctuations are indeed enhanced by the long-range interaction via the formation of the Wigner crystal, although such enhancement is obscured in the single-particle spectrum.

§5. Summary

We have investigated the effect of the orbital degeneracy and the band splitting on the low-energy dynamical properties of 1D quantum liquids in a metallic phase. The single-particle spectrum and

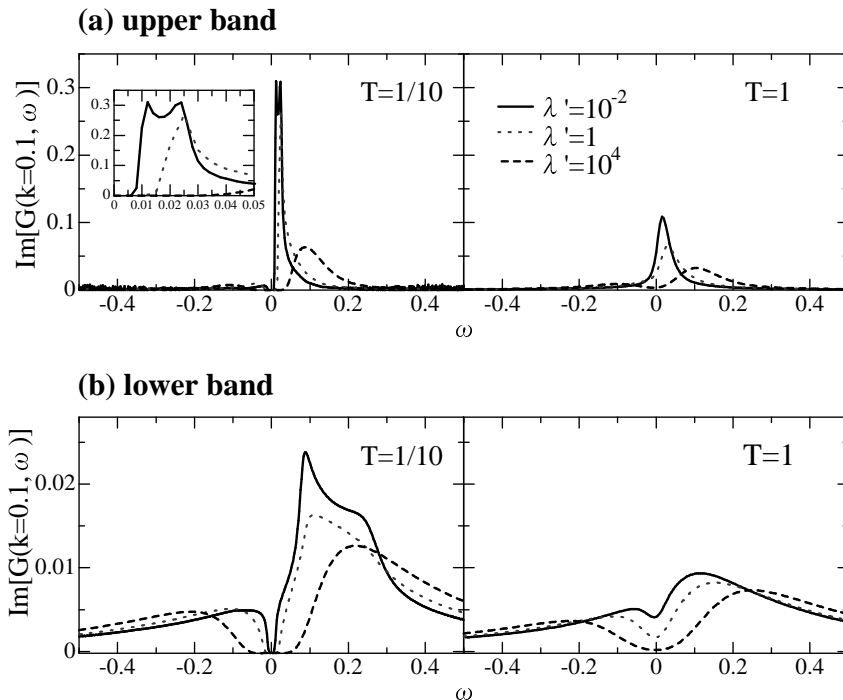


Fig. 7. Single-particle spectrum for the model with short as well as the long-range interaction. The band splitting $\Delta \simeq 0.6$, $\tilde{v}_s \simeq 2.6$, $\tilde{v}_{so} \simeq 0.25$.

the dynamical spin susceptibility have been calculated by exploiting the bosonization techniques. For the multicomponent TL liquid with the short-range interaction, we have found that the spectral function is affected considerably by the orbital degeneracy as well as the band splitting, leading to characteristic features of the profile which are quite contrasted to those expected for the Fermi liquid. The effects of the long-range interaction have also been discussed. It has been found that the charge fluctuations are suppressed while the internal spin and orbital fluctuations are enhanced by the long-range interaction via the formation of the Wigner crystal. However, the enhanced spin fluctuations are hindered in the single-particle spectrum by the almost frozen charge degrees of freedom. It may be interesting to experimentally check whether such enhanced spin fluctuations can be indeed observed for 1D correlated electron systems, such as the carbon nanotube, etc, for which the long-range interaction plays an important role.

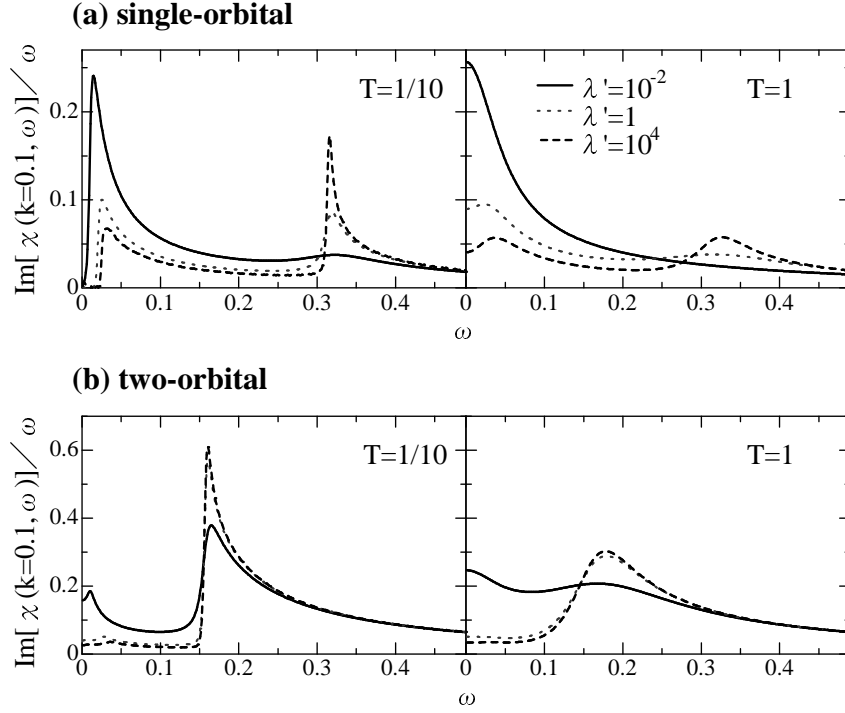


Fig. 8. Spin susceptibility with the short as well as the long-range interaction.

Acknowledgements

This work was partly supported by a Grant-in-Aid from the Ministry of Education, Science, Sports and Culture of Japan. A part of computations was done at the Supercomputer Center at the Institute for Solid State Physics, University of Tokyo and Yukawa Institute Computer Facility. A. K. was supported by Japan Society for the Promotion of Science.

Appendix

The p -dependence of $\alpha(p)$ and $y(p)$ is obtained as,

$$\tan[2\alpha(p)] = \frac{2\Delta v}{v_1} (y(p) - y(p)^{-1})^{-1},$$

$$y^2 = \frac{K_c(p)^{-2} + 1}{K_o^{-2} + 1},$$

and the TL parameters, $K_c(p)$, $v_c(p)$, K_o and v_o , are given by

$$K_c(p) = [1 + 4U(p)a_0/\pi v_1 - Va_0/\pi v_1]^{-1/2},$$

$$K_o = [1 - Va_0/\pi v_1]^{-1/2},$$

$$v_c(p) = v_1 [1 + 4U(p)a_0/\pi v_1 - Va_0/\pi v_1]^{1/2},$$

$$v_o = v_1 [1 - Va_0/\pi v_1]^{1/2},$$

where we have introduced $v_1=[v_F^{(1)}+v_F^{(2)}]/2$ and $\Delta v=[v_F^{(1)}-v_F^{(2)}]/2$. Here V is the on-site Coulomb interaction.

Furthermore, the parameters $\tilde{v}_\nu(p)$ and $\tilde{K}_\nu(p)$ ($\nu=c,o$) in the diagonalized Hamiltonian (9) are given by,

$$\begin{aligned}\tilde{v}_c^2(p) &= \left\{ \frac{v_c(p)}{K_c(p)} \xi_1(p)^2 + \frac{v_o}{K_o} \xi_2(p)^2 + 2\Delta v \xi_1(p) \xi_2(p) \right\} \\ &\quad \times \left\{ v_c(p) K_c(p) \xi_1(p)^2 + v_o K_o \xi_3(p)^2 + 2\Delta v \xi_1(p) \xi_3(p) \right\}, \\ \tilde{v}_o^2(p) &= \left\{ \frac{v_c(p)}{K_c(p)} \xi_3(p)^2 + \frac{v_o}{K_o} \xi_1(p)^2 - 2\Delta v \xi_1(p) \xi_3(p) \right\} \\ &\quad \times \left\{ v_c(p) K_c(p) \xi_2(p)^2 + v_o K_o \xi_1(p)^2 - 2\Delta v \xi_1(p) \xi_2(p) \right\}, \\ \tilde{K}_c^2(p) &= \frac{v_c(p) K_c(p) \xi_1(p)^2 + v_o K_o \xi_3(p)^2 + 2\Delta v \xi_1(p) \xi_3(p)}{\frac{v_c(p)}{K_c(p)} \xi_1(p)^2 + \frac{v_o}{K_o} \xi_2(p)^2 + 2\Delta v \xi_1(p) \xi_2(p)}, \\ \tilde{K}_o^2(p) &= \frac{v_c(p) K_c(p) \xi_2(p)^2 + v_o K_o \xi_1(p)^2 - 2\Delta v \xi_1(p) \xi_2(p)}{\frac{v_c(p)}{K_c(p)} \xi_3(p)^2 + \frac{v_o}{K_o} \xi_1(p)^2 - 2\Delta v \xi_1(p) \xi_3(p)}.\end{aligned}$$

-
- [1] S. Tomonaga: Prog. Theor. Phys. **5** (1950) 544.
 - [2] J. M. Luttinger: J. Math. Phys. **4** (1963) 1154.
 - [3] F. D. M. Haldane: Phys. Rev. Lett. **45** (1980) 1358.
 - [4] C. Kim, A. Y. Matsuura, Z. -X. Shen, N. Motoyama, H. Eisaki, S. Uchida, T. Tohyama and S. Maekawa: Phys. Rev. Lett. **77** (1996) 4054; C. Kim, Z. -X. Shen, N. Motoyama, H. Eisaki, S. Uchida, T. Tohyama and S. Maekawa: Phys. Rev. B **56** (1997) 15589.
 - [5] K. Kobayashi, T. Mizokawa and A. Fujimori: Phys. Rev. Lett. **80** (1998) 3121.
 - [6] M. Takigawa, N. Motoyama, H. Eisaki and S. Uchida: Phys. Rev. Lett. **76** (1996) 4612; M. Takigawa, O. A. Starykh, A. W. Sandvik and R. R. P. Singh: Phys. Rev. B **56** (1997) 13681.
 - [7] G. Chaboussant, Y. Fagot-Revurat, M. -H. Julien, M. E. Hanson, C. Berthier, M. Horvatic, L. P. Lévy and O. Piovesana: Phys. Rev. Lett. **80** (1998) 2713.
 - [8] T. Goto, Y. Fujii, Y. Shimaoka, T. Maekawa and J. Arai: Physica B **284-288** (2000) 1611.
 - [9] S. Sachdev: Phys. Rev. B **50** (1994) 13006.
 - [10] R. Chitra and T. Giamarchi: Phys. Rev. B **55** (1997) 5816.
 - [11] A. Kawaguchi, T. Fujii and N. Kawakami: J. Phys. Soc. Jpn. **69** (2000) 3055
 - [12] E. Axtell, T. Ozawa, S. Kauzlarich and R. R. P. Singh: J. Solid State Chem. **134** (1997) 423.
 - [13] M. Isobe and Y. Ueda: J. Phys. Soc. Jpn. **65** (1996) 1178.
 - [14] Y. Fujii, H. Nakao, T. Yosihama, M. Nishi, K. Nakajima, K. Kakurai, M. Isobe, Y. Ueda and H. Sawa: J. Phys. Soc. Jpn. **66** (1997) 326.
 - [15] H. Smolinski, C. Gros, W. Weber, U. Peuchert, G. Roth, M. Weiden and C. Geibel: Phys. Rev. Lett. **80** (1998) 5164.
 - [16] H. Seo and H. Fukuyama: J. Phys. Soc. Jpn. **67** (1998) 2602.

- [17] P. Thalmeier and P. Fulde: *Europhys. Lett.* **44** (1998) 242.
- [18] M. V. Mostovoy and D. I. Khomskii: *Solid State Commun.* **113** (2000) 159.
- [19] B. Sutherland: *Phys. Rev. B* **12** (1975) 3795.
- [20] I. Affleck: *Nucl. Phys. B* **265** (1986) 409.
- [21] A. G. Izergin, V. E. Korepin and N. Y. Reshetikhin: *J. Phys. A* **22** (1989) 2615.
- [22] T. Itakura and N. Kawakami: *J. Phys. Soc. Jpn.* **64** (1995) 2321.
- [23] P. Azaria, A. O. Gogolin, P. Lecheminant and A. A. Nersesyan: *Phys. Rev. Lett.* **83** (1999) 624; P. Azaria, E. Boulat and P. Lecheminant: *Phys. Rev. B* **61** (2000) 12112.
- [24] Y. Tsukamoto, N. Kawakami, Y. Yamashita and K. Ueda: *Physica B* **281-282** (2000) 540.
- [25] C. Itoi, S. Qin and I. Affleck: *Phys. Rev. B* **61** (2000) 6747.
- [26] S. K. Pati, R. R. P. Singh and D. I. Khomskii: *Phys. Rev. Lett.* **81** (1998) 5406.
- [27] Y. Yamashita, N. Shibata and K. Ueda: *J. Phys. Soc. Jpn.* **69** (2000) 242; *Physica B* **281-282** (2000) 542.
- [28] Z. N. C. Ha and F. D. M. Haldane: *Phys. Rev. Lett.* **73** (1994) 2887.
- [29] Y. Kato and Y. Kuramoto: *J. Phys. Soc. Jpn.* **65** (1996) 1622; Y. Kato: *Phys. Rev. Lett.* **81** (1998) 5402.
- [30] M. Arikawa, Y. Saiga and Y. Kuramoto: *Phys. Rev. Lett.* **86** (2001) 3096.
- [31] H. J. Schulz: *Phys. Rev. Lett.* **71** (1993) 1864.
- [32] H. Otani and T. Ogawa: *Phys. Rev. B* **54** (1996) 4540.
- [33] Y. Tsukamoto and N. Kawakami: *J. Phys. Soc. Jpn.* **69** (2000) 149.
- [34] P. Schlottmann: *Phys. Rev. B* **36** (1987) 5177.
- [35] P. A. Bares and G. Blatter: *Phys. Rev. Lett.* **64** (1990) 2567.
- [36] N. Kawakami and S. -K. Yang: *Phys. Rev. Lett.* **65** (1990) 2309.
- [37] M. Ogata and H. Shiba: *Phys. Rev. B* **41** (1990) 2326.
- [38] S. Sorella and A. Parola: *J. Phys.: Condens. Matter* **4** (1992) 3589; *Phys. Rev. Lett.* **76** (1996) 4604; *Phys. Rev. B* **57** (1998) 6444.
- [39] V. Meden and K. Schönhammer: *Phys. Rev. B* **46** (1992) 15753; K. Schönhammer and V. Meden: *Phys. Rev. B* **47** (1993) 16205.
- [40] N. Nakamura and Y. Suzumura: *Prog. Theor. Phys.* **97** (1997) 163; *Prog. Theor. Phys.* **98** (1997) 29.